

Optimization of User Equipment Random Access Delay in LEO Satellite Communication Systems via Synchronization Signal Block Periodicity

A Thesis
Presented to
The Academic Faculty

by

Po-Yu Yen

In Partial Fulfillment
of the Requirements for the Degree
Master of Science in the
Graduate Institute of Communication Engineering

National Taiwan University

July 2025

ABSTRACT

Low Earth Orbit (LEO) satellite network has been a promising technology due to the wide spread coverage area and high data throughput. However, with the high speed of satellites, frequent handover is unavoidable for user equipments (UEs) on the ground, causing significant interruption time and signaling overhead. Thus, we introduce a quasi-earth-fixed satellite beam scheme to solve the continually handover from the UEs at the cell edge. In this scheme, we allocate the satellite beams to the ground cells in order to maximize overall throughput. After that, we also propose a UE cell selection algorithm, which base on both position information and UE measurement.

TABLE OF CONTENTS

ABSTRACT	ii
LIST OF TABLES	v
LIST OF FIGURES	vi
CHAPTER 1 INTRODUCTION	1
CHAPTER 2 BACKGROUND AND RELATED WORK	4
2.1 Random Access Procedure	4
2.2 Synchronization Signal Block	4
2.2.1 Components of SSB	4
2.2.2 SSB Configuration	5
2.2.3 SSB in LEO Satellite Network	5
2.3 Related Work	6
CHAPTER 3 SYSTEM MODEL	7
3.1 System Overview	7
3.2 Channel Model	8
3.2.1 Free Space Path Loss	8
3.2.2 Shadowed-Rician Fading Channel	8
3.2.3 Antenna Radiation Pattern	9
3.2.4 UE Received Power	9
3.3 Joint Power-Periodicity Optimization on SSB	9
3.3.1 Synchronization Signal Block Periodicity	10
3.3.2 Satellite Power Budget	10
3.4 UE Cell Searching Delay	10
3.5 Problem Formulation	11
CHAPTER 4 PROPOSED ALGORITHM	13
4.1 Taylor Expansion on Objective Function	13
4.2 Result	15
4.3 Future Work	16

CHAPTER 5 PERFORMANCE EVALUATION	17
5.1 Simulation Setup	17
5.2 Simulation Results	17
CHAPTER 6 CONCLUSION AND FUTURE WORK	18
REFERENCES	19

LIST OF TABLES

1	Comparison of different solution method	16
---	---	----

LIST OF FIGURES

1	Time to handover for min/max cell diameter and varying UE speed	3
2	Illustration of SSB configuration.	5
3	Illustration of satellite beams and cells.	7
4	Illustration of random access delay at \mathcal{S}_i -th epoch	11
5	Taylor series expansion diagram flow	13

CHAPTER 1

INTRODUCTION

Non-terrestrial networks (NTNs) have emerged as a promising solution for next-generation communication systems. They enable network connectivity in areas that are beyond the reach of conventional terrestrial infrastructure. In particular, in natural environments such as forests, oceans, and deserts, terrestrial networks are not only impractical to deploy due to the sparse distribution of user equipment (UE) but also environmentally unsustainable, as their construction may cause significant ecological disturbance. A variety of platforms can be employed to provide network services in NTNs, including geostationary Earth orbit (GEO), medium Earth orbit (MEO), and low Earth orbit (LEO) satellites, as well as unmanned aerial vehicles (UAVs) and high-altitude drones. Among these, LEO satellite systems have attracted the most attention in recent research. Operating at altitudes ranging approximately from 500 km to 2000 km, LEO satellites offer global coverage comparable to GEO and MEO systems but with significantly shorter propagation distances. This feature leads to reduced latency and lower propagation loss, thereby improving the received signal-to-noise ratio (SNR) and enhancing overall data throughput performance.

Practically, each LEO satellite covers a vast service area to achieve global coverage. However, transmitting signals using a single beam encompassing the entire coverage area is impractical, as the resultant SNR at the ground UE would be insufficient. To ensure the required received SNR at the UE side, beamforming techniques are employed to concentrate the beam energy and illuminate specific spots, which correspond to cells within the overall coverage area. By employing this approach, the entire coverage area is effectively partitioned into tens or even hundreds of smaller cells. Consequently, a critical challenge arises regarding the optimal allocation of resources among these cells in order to maximize overall network performance and efficiency.

Resource allocation in beam hopping has been widely studied as a key issue in LEO satellite communication networks. Beam hopping refers to the technique where active beams on a LEO satellite sequentially serve different cells during different time slots, thereby providing coverage to the entire service area. In this context, optimizing power allocation and beam pattern scheduling to maximize overall system throughput has been extensively explored [1]. Additionally, latency optimization through power allocation and beam scheduling has also garnered

significant attention [2]. However, to the best of our knowledge, existing research has not addressed the problem of initial access delay within the beam hopping framework.

In the 3rd Generation Partnership Project (3GPP) 5G network architecture, Ultra-Reliable and Low-Latency Communications (URLLC) has been identified as a key service category, enabling latency-critical applications such as smart manufacturing, emergency response, and real-time media streaming. Although LEO satellite communication provides the shortest propagation delay among satellite orbit types compared to MEO and GEO systems, the overall end-to-end connection time between a satellite and a ground UE remains relatively large due to factors such as long transmission distances and complex link establishment procedures. Particularly in the initial cell search phase, the process is further complicated in LEO satellite communications due to the aforementioned cell structure, which impacts connection setup latency and resource management.

Several studies have investigated initial access delay in terrestrial networks, particularly in millimeter-wave scenarios, which are key technologies in New Radio (NR) and beyond networks. For example, [3] focuses on maximizing the number of reference signals received per time slot while ensuring fairness and limiting the number of time slots per access round. Another work [4] examines initial access delay in autonomous vehicle networks, identifying the main challenge as the selection of the transmit/receive (Tx/Rx) beam pair in terrestrial systems. However, the initial access search process in LEO satellite networks presents greater complexity due to the unique characteristics of satellite communication and the multi-cell beam structure, making the challenge more intricate than in terrestrial networks.

There are two primary factors influencing the delay in the initial cell search phase in LEO satellite communications: the number of simultaneously active beams and the transmitted power of the synchronization signal block (SSB). Firstly, supporting multiple active beams enables a satellite to serve multiple cells concurrently. Combined with the beam hopping technique, these active beams sequentially illuminate different cells in distinct time slots to cover the entire service area. Implementing such multi-beam service requires deploying a large-scale phased antenna array onboard the satellite, whose physical size directly impacts both the cost and engineering complexity of the satellite design. Moreover, an increased number of simultaneously active beams means that the available power must be divided among more beams, linking closely to the second factor. The transmitted power of the SSB significantly affects the success rate of connection

establishment between the satellite and user equipment (UE). Insufficient transmitted power may cause the UE to incorrectly decode the signal, leading to increased connection latency. Conversely, excessive transmitted power is inefficient since the SSB is a control signal; boosting its power does not yield proportional gains as it would for data transmission. Furthermore, because the satellite's total transmitted power mainly relies on onboard solar panels with limited energy supply, power must be managed efficiently to ensure reliable and sustainable operation.

Cell Diameter Size (km)	UE Speed (km/hr)	Satellite Speed (km/s)	Time to HO (s)
50 (lower bound)	+500	7.56 (NOTE 1)	6.49
	-500		6.74
	+1200		6.33
	-1200		6.92
	Neglected		6.61
1000 (upper bound)	+500	7.56 (NOTE 1)	129.89
	-500		134.75
	+1200		126.69
	-1200		138.38
	Neglected		132.28

Figure 1: Time to handover for min/max cell diameter and varying UE speed

CHAPTER 2

BACKGROUND AND RELATED WORK

2.1 *Random Access Procedure*

The random access procedure in 5G is a critical mechanism that allows a User Equipment (UE) to establish initial uplink synchronization and connect to the network (gNB). The procedure is essential for first-time access, handovers, and re-establishing connections after inactivity or loss of synchronization. Here are some typical steps in contention-based random access:

- Preamble Transmission (Msg1): The UE randomly selects a PRACH (Physical Random Access Channel) preamble and transmits it to the gNB. This “signature” indicates the UE’s request for network access.
- Random Access Response (Msg2): The gNB detects the preamble and responds with a Random Access Response (RAR), which includes timing adjustment, a temporary identity, and an uplink resource grant. This enables the UE to align its timing with the network and prepare for further communication.
- RRC Connection Request (Msg3): Using the granted resources, the UE sends a connection request, which includes its identity and the reason for establishing the connection, such as initial access or handover.
- Contention Resolution (Msg4): The gNB sends a contention resolution message confirming which UE has successfully completed the random access. If multiple UEs used the same preamble, only the correct one will be acknowledged, resolving the contention.

2.2 *Synchronization Signal Block*

2.2.1 Components of SSB

The Synchronization Signal Block (SSB) in 5G New Radio (NR) is a critical structure for initial access between the user equipment (UE) and the base station (gNB). Each SSB is composed of three main elements:

- Primary Synchronization Signal (PSS): The PSS enables the UE to obtain symbol timing and perform coarse frequency synchronization. It allows the

UE to find the starting point of a radio frame and resolves the physical layer cell identity group.

- Secondary Synchronization Signal (SSS): The SSS complements PSS by providing additional information to finalize the cell identification and determines the frame timing, which refines synchronization accuracy for the UE.
- Physical Broadcast Channel (PBCH): The PBCH conveys essential cell-specific information, including system configuration parameters (such as the System Frame Number), which the UE needs for further connection setup after synchronization.

These components jointly allow the UE to perform downlink synchronization, cell identification, and to decode key system information for network access.

2.2.2 SSB Configuration

A series of SSBs called *SSB burst* are sent in a half frame (5ms), the number of SSBs in a SSB burst is determined depends on the carrier frequency and the subcarrier spacing of the transmitted signals. Each cell has a SSB periodicity, defined as the time interval the SSB burst be transmitted to the cell, as shown in Figure 2.

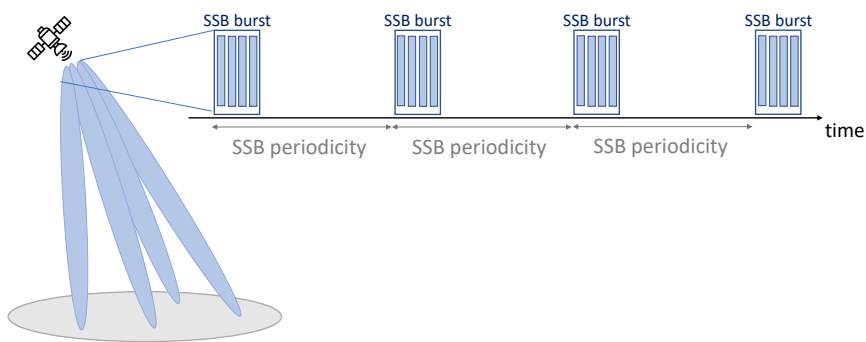


Figure 2: Illustration of SSB configuration.

2.2.3 SSB in LEO Satellite Network

In terrestrial network (TN), the base station (gNB) transmits SSBs periodically in time and across different spatial directions through beam sweeping, enabling the UE to detect the best SSB and select the optimal beam for communication. In NTN, the SSBs have the same function but the coverage area of each satellite is much bigger than TN, which means each satellite has to provide service to more cells. Moreover, the long distance from satellite to ground and the power budget

of each satellite forces us to properly allocate the power of the SSB. Thus, it is essential for us to manage the SSB transmitted power and the periodicity of each cell.

2.3 Related Work

CHAPTER 3

SYSTEM MODEL

3.1 System Overview

This chapter introduces the LEO satellite communication system, as illustrated in Figure 3. We consider one of the satellites in the LEO satellite communication system. It consists of M beams, represented by $\mathcal{M} = \{m \mid m = 1, 2, \dots, M\}$. In the coverage area of the satellite, it contains K cells, indexed by $\mathcal{K} = \{k \mid k = 1, 2, \dots, K\}$. To achieve optimal coverage and minimize overlap, all ground cells are arranged in a regular hexagonal grid, ensuring uniform cell size. There are U user equipments (UEs) in the coverage area, indexed by $\mathcal{U} = \{u \mid u = 1, 2, \dots, U\}$.

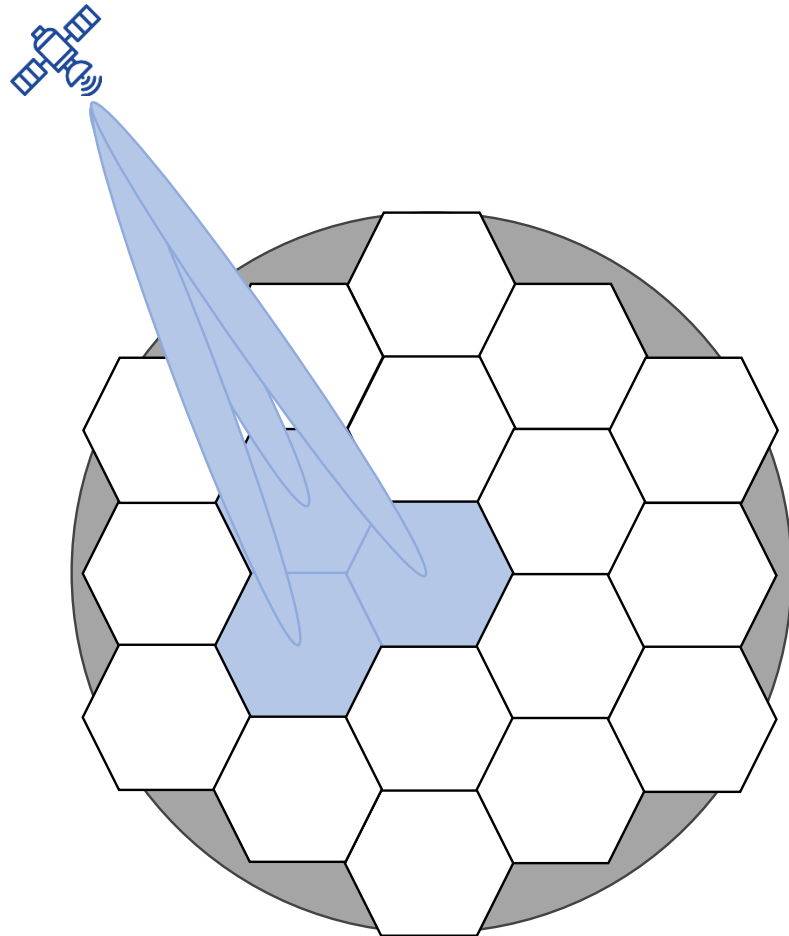


Figure 3: Illustration of satellite beams and cells.

We define a short time T^{slot} as the time duration of a time slot, and T^{total} as the total time that the satellite serves the area. Thus, there are T^{total}/T^{slot} time

slots in total service time, denoted as $\mathcal{T} = \{t \mid t = 1, 2, \dots, T^{total}/T^{slot}\}$.

In this thesis, we adopt the quasi-earth-fixed scheme. Unlike the earth-moving cell scheme—where the coverage areas of satellite beams move as the LEO satellites orbit—this approach directs satellite beams so that each beam consistently covers the same geographical cell for a given period. Thus, the coverage area of each satellite beam remains fixed relative to the ground during that interval. Throughout, we assume each satellite beam is oriented toward the center of its designated cell.

The locations of UEs wishing to access the network are assigned randomly within their corresponding cells, and the population of each cell are generated according to area population density statistics.

3.2 *Channel Model*

3.2.1 Free Space Path Loss

In the LEO satellite system, the free space path loss from the satellite to cell k is expressed as follows [5]:

$$L_k = \left(\frac{\lambda}{4\pi d_k} \right)^2 \quad (3.1)$$

where λ is the wavelength, and d_k is the distance between the satellite and the center of the k -th cell.

3.2.2 Shadowed-Rician Fading Channel

The shadowed-Rician fading model is suitable for satellite communication systems because it accurately reflects the physical propagation environment, capturing both the presence of a strong line-of-sight (LoS) signal and the effects of shadowing from obstacles [6]. Let h_k denote the channel gain between the satellite and the k -th cell. The cumulative distribution function (CDF) of the channel gain is:

$$F_{h_k}(x) = K \sum_{n=0}^{\infty} \frac{(m)_n \delta^n (2b)^{1+n}}{(n!)^2} \zeta \left(1 + n, \frac{x}{2b} \right) \quad (3.2)$$

where $K = \left(\frac{2bm}{2bm + \Omega} \right)^m / 2b$, $\delta = \Omega / (2bm + \Omega) / 2b$, Ω is the average power of the LoS component, $2b$ is the average power of the multipath component except the LoS component, and m is the Nakagami parameter. $\Gamma(\cdot)$ is the Gamma function, and the Pochhammer symbol is defined as $(x)_n = \Gamma(x+n)/\Gamma(x)$. The lower incomplete Gamma function is defined as $\zeta(a, x) = \int_0^x t^{a-1} \exp(-t) dt$.

3.2.3 Antenna Radiation Pattern

We introduce the antenna radiation pattern in [7]:

$$G(\phi_{k,u}) = G_{max} \left[\frac{J_1(\mu(\phi_{k,u}))}{2\mu(\phi_{k,u})} + 36 \frac{J_3(\mu(\phi_{k,u}))}{\mu(\phi_{k,u})^3} \right]^2 \quad (3.3)$$

where $\phi_{k,u}$ is the boresight angle between the user position and the cell center with respect to the satellite, G_{max} is the maximum antenna gain, $\mu(\phi)$ is defined as $2.07123 \cdot \sin(\phi) / \sin(\phi_{3dB})$, ϕ_{3dB} is the 3 dB half-power beamwidth angle of the antenna, and $J_1(\cdot)$, $J_3(\cdot)$ are the Bessel functions of the first kind of orders 1 and 3, respectively.

3.2.4 UE Received Power

In this thesis, the transmitted power of each beam is fixed during one epoch. The transmitted power to the k -th cell at the \mathcal{S}_i -th epoch is denoted as $P_k[\mathcal{S}_i]$. In the \mathcal{S}_i -th epoch, the received power of the u -th user in the k -th cell at the t -th time slot $\hat{P}_{k,u}[t]$ can be calculated as follows:

$$\hat{P}_{k,u}[t] = P_k[\mathcal{S}_i] \cdot L_k \cdot h_k \cdot G(\phi_{k,u}) \quad (3.4)$$

3.3 Joint Power-Periodicity Optimization on SSB

In this section, we will discuss how the satellite beam transmitted power and the SSB periodicity affect UE cell search delay and formulate an optimization problem. During the total service time, it is essential to adjust the satellite beam transmitted power and the SSB periodicity because the system environment changes in real-time. The most significant change is the elevation angle of the satellite. It affects not only the transmission distance, but also the channel fading effect. However, if we adjust the power and periodicity too frequently, the computation complexity rises and the signaling overhead increases. Thus, we adjust the satellite beam transmitted power and the SSB periodicity in a certain number of time slots, defined as an epoch. We define one epoch equals to N time slots, so there are $T^{total}/T^{slot}/N$ epochs in total. The set of all epochs within the service duration is represented as $\tilde{\mathcal{S}} = \{\mathcal{S}_i \mid i = 0, 1, 2, \dots, (T^{total}/T^{slot}/N - 1)\}$, where each epoch S_i encompasses the time slots from iN to $(i+1)N - 1$. By adjusting system parameters only at epoch boundaries, this approach balances real-time responsiveness against the complexity and signaling overhead associated with too frequent updates, ensuring system stability and efficient resource allocation throughout the mission duration.

3.3.1 Synchronization Signal Block Periodicity

During the total service time, the satellite transmits SSBs to the serving cells at specific time intervals, depending on the SSB periodicity configured for each cell. With longer SSB periodicity, the satellite beam has more time slots to serve other cells, and can allocate more power to each SSB signal. Thus, we adjust the SSB periodicity every epoch. During each epoch, the SSB periodicity of each cell is fixed. We then define the SSB periodicity of the cell k at the \mathcal{S}_i -th epoch as the number of slots between two consecutive SSBs that transmit to the k -th cell, denoted as $\theta_k[\mathcal{S}_i]$. Since there are at most M beams serving the cells in one satellite and one beam can only transmit one SSB to a cell in a time slot, we must insure that there are enough time slots to transmit all SSBs in one cycle. That is,

$$\sum_k \frac{1}{\theta_k[\mathcal{S}_i]} \leq M, \quad \forall \mathcal{S}_i \in \tilde{\mathcal{S}} \quad (3.5)$$

3.3.2 Satellite Power Budget

In LEO satellite communication systems, satellites primarily rely on solar power for data transmission. Each satellite has a specific power budget, determined by the amount of solar energy it can harvest. Since the distance between space and ground is typically several hundred kilometers, transmitted signals must be strong enough to achieve the minimum signal-to-noise ratio (SNR) required on the user equipment (UE) side. Therefore, the efficient allocation of power resources to each beam under a limited power budget is a critical topic in LEO satellite communication system design. We define a power budget for the satellite. Let $P_k[\mathcal{S}_i]$ denote the transmitted power to the k -th cell at epoch \mathcal{S}_i . The aggregate transmit power of all beams on the satellite must satisfy:

$$\sum_m \frac{P_k[\mathcal{S}_i]}{\theta_k[\mathcal{S}_i]} \leq P^{total}, \quad \forall \mathcal{S}_i \in \tilde{\mathcal{S}} \quad (3.6)$$

where P^{total} is the maximum transmit power for a satellite in one time slot.

3.4 UE Cell Searching Delay

The cell searching delay $\alpha_u[\mathcal{S}_i]$ for the u -th UE is a random variable, defined as the time duration between the start of SSB measurement and the successful reception of SSB at the \mathcal{S}_i -th epoch, as shown in Figure 4. $\alpha_u[\mathcal{S}_i]$ can be decomposed into two parts: $\beta_u[\mathcal{S}_i]$ (initial waiting time at the \mathcal{S}_i -th epoch) and $\gamma_u[\mathcal{S}_i]$ (additional delay due to failed attempts at the \mathcal{S}_i -th epoch). $\beta_u[\mathcal{S}_i]$ is a random variable that represents the time from the start of SSB measurement to the arrival of the first SSB, and $\gamma_u[\mathcal{S}_i]$ is another random variable that represents the

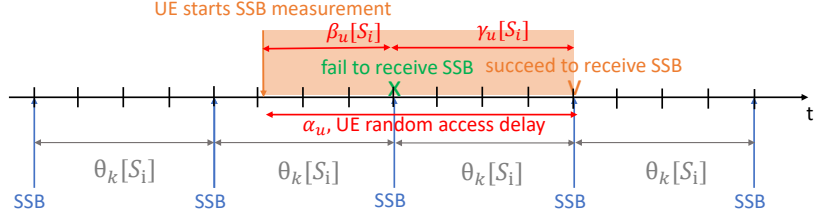


Figure 4: Illustration of random access delay at \mathcal{S}_i -th epoch

time from the first SSB arrival to the successful SSB reception. Since the UE can start SSB measurement at any time, $\beta_u[\mathcal{S}_i]$ follows uniform distribution from 0 to $\theta_k[\mathcal{S}_i]$, where k represents the serving cell of u . $\gamma_u[\mathcal{S}_i]$ is a multiple of $\theta_k[\mathcal{S}_i]$, depending on the number of SSB reception failures $Q_u[\mathcal{S}_i]$, which is a discrete random variable. If the received SSB power at the t -th time slot $\hat{P}_{m,u}[t]$ is less than the threshold P^{th} , the UE fails to measure SSB. The probability that the received SSB power is less than P^{th} at the t -th time slot is denoted as $R_u[t]$. The mathematical formulation is as follows:

$$\alpha_u[\mathcal{S}_i] = \beta_u[\mathcal{S}_i] + \gamma_u[\mathcal{S}_i] \quad (3.7)$$

$$F_{\beta_u[\mathcal{S}_i]}(x) = \begin{cases} \frac{x}{\theta_k[\mathcal{S}_i]}, & 0 \leq x < \theta_k[\mathcal{S}_i] \\ 1, & x \geq \theta_k[\mathcal{S}_i] \\ 0, & \text{otherwise} \end{cases} \quad (3.8)$$

$$\gamma_u[\mathcal{S}_i] = Q_u[\mathcal{S}_i] \cdot \theta_k[\mathcal{S}_i] \quad (3.9)$$

where $F_{\beta_u[\mathcal{S}_i]}(x)$ is the CDF of $\beta_u[\mathcal{S}_i]$. To calculate the Probability Mass Function (PMF) of $Q_u[\mathcal{S}_i]$, we denote the u -th UE fails to measure n SSBs at t_1, t_2, \dots, t_n time slots, and successfully receives SSB at time slot t_{n+1} . The PMF of $Q_u[\mathcal{S}_i]$ can be express as follows:

$$\Pr\{Q_u[\mathcal{S}_i] = n\} = (1 - R_u[t_{n+1}]) \prod_{i=1}^n R_u[t_i] \quad (3.10)$$

$R_u[t]$ can be expressed by F_{h_k} as follows:

$$\begin{aligned} R_u[t] &= \Pr\{\hat{P}_{k,u}[t] < P^{th}\} \\ &= \Pr\{h_k < \frac{P^{th}}{P_k[\mathcal{S}_i] \cdot L_k \cdot G(\phi_{m,u})}\} \\ &= F_{h_k}\left(\frac{P^{th}}{P_k[\mathcal{S}_i] \cdot L_k \cdot G(\phi_{m,u})}\right) \end{aligned} \quad (3.11)$$

3.5 Problem Formulation

This section formulates the optimization problem based on recent 3GPP standardization discussions. The main challenge is to provide SSBs to as many cells as

possible with limited satellite power. Extending the SSB periodicity for some cells increases UE random access delay, but it saves more power so that there would be other cells to be served. On the other hand, shortening the SSB periodicity reduces the UE cell searching delay, but the serving cells might be less because of the power budget. The transmitted SSB power also affects the success probability of the cell searching delay. The trade-off among power allocation, SSB periodicity, and UE cell searching delay is modeled as follows:

$$\min_{P, \theta} \sum_u \sum_{\mathcal{S}_i \in \tilde{\mathcal{S}}} \mathbb{E}[\alpha_u[\mathcal{S}_i]] \quad (3.12a)$$

subject to

$$P_k[\mathcal{S}_i] \geq 0, \quad \forall k \in \mathcal{K}, \mathcal{S}_i \in \tilde{\mathcal{S}} \quad (3.12b)$$

$$\theta_k[\mathcal{S}_i] \leq N, \quad \forall k \in \mathcal{K}, \mathcal{S}_i \in \tilde{\mathcal{S}} \quad (3.12c)$$

$$\theta_k[\mathcal{S}_i] \in \mathbb{N}^+, \quad \forall k \in \mathcal{K}, \mathcal{S}_i \in \tilde{\mathcal{S}} \quad (3.12d)$$

$$\sum_k \frac{P_k[\mathcal{S}_i]}{\theta_k[\mathcal{S}_i]} \leq P^{total}, \quad \forall \mathcal{S}_i \in \tilde{\mathcal{S}} \quad (3.12e)$$

$$\sum_k \frac{1}{\theta_k[\mathcal{S}_i]} \leq M, \quad \forall \mathcal{S}_i \in \tilde{\mathcal{S}} \quad (3.12f)$$

where \mathbb{N}^+ is the set with all positive integers. The mathematical formula between transmitted power and received power is described in equation (3.4). And the mathematical derivation between the received power $\hat{P}_{m,u}[t]$, $\theta_k[s]$ and $\alpha_u[s]$ is described from equation (3.7) to equation (3.11).

CHAPTER 4

PROPOSED ALGORITHM

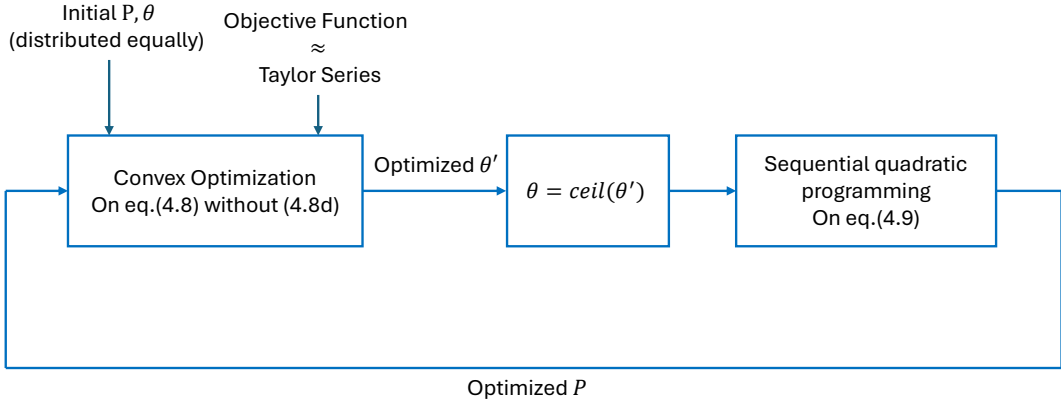


Figure 5: Taylor series expansion diagram flow

4.1 Taylor Expansion on Objective Function

The flow diagram of the algorithm is shown in Figure 5. In this method, we use Taylor expansion on F_{h_k} to approximate the non-linear term into linear term. Below are the calculations:

$$\begin{aligned}
 F(x) &= K \sum_{n=0}^{\infty} \frac{(m)_n d^n (2b)^{tn}}{(n!)^2} \zeta(1+n, \frac{x}{2b}) \\
 &= K \sum_{n=0}^{\infty} \frac{(m)_n d^n (2b)^{tn}}{(n!)^2} \int_0^{\frac{x}{2b}} t^n \exp(-t) dt
 \end{aligned} \tag{4.1}$$

$$\frac{dF(x)}{dx} = K \sum_{n=0}^{\infty} \frac{(m)_n d^n (2b)^{tn}}{(n!)^2} \left(\frac{x}{2b}\right)^n \exp\left(\frac{x}{2b}\right) \cdot \frac{1}{2b} \tag{4.2}$$

Given a real number a , the first order Taylor series of a real function $f(x)$ can be expressed as:

$$f(x) \approx f(a) + f'(a) \cdot (x - a) \tag{4.3}$$

Then the expectation of the number of SSB reception failures $Q_u[S_i]$ can be expressed as follows:

$$\begin{aligned} \mathbb{E}[Q_u[S_i]] &= \frac{F\left(\frac{P_k^{\text{th}}}{P_k \cdot L_k}\right)}{1 - F\left(\frac{P_k^{\text{th}}}{P_k \cdot L_k}\right)} \\ &\approx \frac{F(a) + F'(a) \cdot \left(\frac{P_k^{\text{th}}}{P_k \cdot L_k} - a\right)}{1 - [F(a) + F'(a) \cdot \left(\frac{P_k^{\text{th}}}{P_k \cdot L_k} - a\right)]} \end{aligned} \quad (4.4)$$

where k is the cell that the u -th user connected to. The expectation of user cell searching delay can be expressed as follows:

$$\begin{aligned} E[\alpha_u] &= E[\beta_u] + E[\gamma_u] \\ &= E[\beta_u] + E[Q_u] \cdot \theta_k \\ &= \left(\frac{1}{2} + \frac{P_k C + E_k}{P_k(1 - C) - E_k}\right) \theta_k \end{aligned} \quad (4.5)$$

where $C = F(a) - F'(a) \cdot a$, $E_k = \frac{F'(a) P^{\text{th}}}{L_k}$. We introduce the population density of the k -th cell as D_k . Then the expectation of cell searching delay for a UE can be expressed as follows:

$$E[\alpha_u] = \frac{1}{\sum_k D_k} \sum_k D_k \left(\frac{1}{2} + \frac{P_k C + E_k}{P_k(1 - C) - E_k}\right) \theta_k \quad (4.6)$$

We can rewrite the problem from 3.12 as follows:

$$\min_{P, \theta} \frac{1}{\sum_k D_k} \sum_k D_k \left(\frac{1}{2} + \frac{P_k C + E_k}{P_k(1 - C) - E_k}\right) \theta_k \quad (4.7a)$$

$$\text{subject to} \quad (4.7b)$$

$$P_k > 0, \quad \forall k \in \mathcal{K} \quad (4.7c)$$

$$\theta_k \leq N, \quad \forall k \in \mathcal{K} \quad (4.7d)$$

$$\theta_k \in \mathbb{N}^+, \quad \forall k \in \mathcal{K} \quad (4.7e)$$

$$\sum_k \frac{P_k}{\theta_k} \leq P_{\text{total}} \quad (4.7f)$$

$$\sum_k \frac{1}{\theta_k} \leq M \quad (4.7g)$$

Alternating optimization is a widely used strategy for non-convex problems that involve multiple variables or mixed types of parameters. The core idea is to decompose the original challenging joint optimization into two or more easier subproblems, which are solved iteratively. In our problem, we first fix the power allocation P and optimize the SSB periodicity θ . Then, we fix the SSB periodicity θ and

optimize the power allocation P . This process repeats until convergence. Here we use alternating optimization to separate equation (4.7) into two subproblems. With fixed power, we optimize SSB periodicity:

$$\min_{\theta} \frac{1}{\sum_k D_k} \sum_k D_k \left(\frac{1}{2} + \frac{P_k C + E_k}{P_k(1 - C) - E_k} \right) \theta_k \quad (4.8a)$$

$$\text{subject to} \quad (4.8b)$$

$$\theta_k \leq N, \quad \forall k \in \mathcal{K} \quad (4.8c)$$

$$\theta_k \in \mathbb{N}^+, \quad \forall k \in \mathcal{K} \quad (4.8d)$$

$$\sum_k \frac{P_k}{\theta_k} \leq P_{\text{total}} \quad (4.8e)$$

$$\sum_k \frac{1}{\theta_k} \leq M \quad (4.8f)$$

And with fixed SSB periodicity, we optimize power:

$$\min_P \frac{1}{\sum_k D_k} \sum_k D_k \left(\frac{1}{2} + \frac{P_k C + E_k}{P_k(1 - C) - E_k} \right) \theta_k \quad (4.9a)$$

$$\text{subject to} \quad (4.9b)$$

$$P_k > 0, \quad \forall k \in \mathcal{K} \quad (4.9c)$$

$$\sum_k \frac{P_k}{\theta_k} \leq P_{\text{total}} \quad (4.9d)$$

For problem (4.8), it satisfies convex optimization problem if we ignore constraint that θ must be integer (4.8d). Thus, we compute the problem (4.8) without constraint (4.8d) by cvx in matlab, and then ceil the θ to make sure all θ satisfy constraint (4.8d).

For problem (4.9), it is not a convex optimization problem. Thus we use sequential quadratic programming (SQP) to calculate the result.

4.2 Result

The result is shown in Table 1. We distribute power and SSB periodicity for all cells equally and minimize θ to reach constraint (4.7g) as our baseline. That is,

$$P_k = P_{\text{total}}/M, \quad \forall k \in \mathcal{K} \quad (4.10)$$

$$\theta_k = K/M, \quad \forall k \in \mathcal{K} \quad (4.11)$$

The gain is calculated as $\frac{(\text{delay of baseline} - \text{delay of proposed method})}{\text{delay of baseline}}$.

Table 1: Comparison of different solution method

	Equally Distributed	Taylor
delay (number of time slots)	18.6805	13.6312
gain	0%	27%

4.3 Future Work

1. I only consider one epoch in my proposed method so far. I am trying to find out the relation between epochs and help me find the better solution.
2. In problem (4.9), SQP does not guarantee global optimal solution. I will figure out if there is any other approach to calculate a better solution.

CHAPTER 5

PERFORMANCE EVALUATION

All figures should be of the same width whenever possible for consistency.

5.1 *Simulation Setup*

We use BONMON [?] to solve the optimization problem. The simulation setup follows that in [?].

5.2 *Simulation Results*

CHAPTER 6

CONCLUSION AND FUTURE WORK

REFERENCES

- [1] L. Chen, L. Wu, E. Lagunas, A. Wang, L. Lei, S. Chatzinotas, and B. Ottersten, “Joint power allocation and beam scheduling in beam-hopping satellites: A two-stage framework with a probabilistic perspective,” *IEEE Transactions on Wireless Communications*, vol. 23, no. 10, pp. 14 685–14 701, 2024.
- [2] S. Guo, L. Zhao, and Y. Cui, “Latency optimization of leo satellite communication systems with beam hopping,” in *2022 IEEE International Conference on Satellite Computing (Satellite)*, 2022, pp. 37–42.
- [3] C.-W. Weng, B. P. S. Sahoo, H.-Y. Wei, and C.-H. Yu, “Directional reference signal design for 5g millimeter wave cellular systems,” *IEEE Transactions on Vehicular Technology*, vol. 67, no. 11, pp. 10 740–10 751, 2018.
- [4] M. N. Ahangar, Q. Z. Ahmed, M. Hafeez, and M. S. Bashir, “Artificial intelligence-aided beam tracking in autonomous vehicles: State of the art and future directions,” *IEEE Transactions on Intelligent Transportation Systems*, vol. 26, no. 11, pp. 18 385–18 403, 2025.
- [5] J. Wang, C. Jiang, L. Kuang, and R. Han, “Satellite multi-beam collaborative scheduling in satellite aviation communications,” *IEEE Transactions on Wireless Communications*, vol. 23, no. 3, pp. 2097–2111, 2024.
- [6] D.-H. Jung, J.-G. Ryu, W.-J. Byun, and J. Choi, “Performance analysis of satellite communication system under the shadowed-rician fading: A stochastic geometry approach,” *IEEE Transactions on Communications*, vol. 70, no. 4, pp. 2707–2721, 2022.
- [7] S.-H. Chen, L.-H. Shen, K.-T. Feng, L.-L. Yang, and J.-M. Wu, “Energy-efficient joint handover and beam switching scheme for multi-leo networks,” in *2024 IEEE 99th Vehicular Technology Conference (VTC2024-Spring)*, 2024, pp. 1–7.